Journal of Chromatography, 89 (1974) 119–130

CHROM. 7177

NON-IDEAL LINE SHAPES IN GAS–LIQUID CHROMATOGRAPHY

SHANG-DA HUANG, JOHN W. WILSON, DAVID J. WILSON and KNOWLES A. OVERHOLSER

Departments of Chemistry and Chemical Engineering, Vanderbilt University, Nashville, Tenn. 37235 (U.S.A.)

(Received September 17th, 1973)

SUMMARY

The effects of velocity and diffusion constant variation along the length of the gas chromatographic column and of the finite rate of mass transport between the moving and stationary phases are examined. Realistic variation of velocity and diffusion constant with pressure does not result in major changes in line shape. Decreasing the rate of adsorption and desorption results in the expected line broadening. The dependence of peak width upon gas inlet velocity is found to be in good agreement with the Van Deemter equation. Frontal analysis is examined, and the effects of varying mass transport coefficients on the shapes of the fronts is computed. The effects of finite sample injection time internal and of non-ideal Henry's law constants are also investigated for the case of pulse injection.

INTRODUCTION

Giddings[1] has thoroughly reviewed the theories of gas–liquid chromatographic (GLC) line shapes, and has presented a very general approach to the subject. Line shapes are determined by eddy diffusion, resistance to mass transport between phases, and molecular diffusion in the vapor phase. These effects are usually combined in an effective diffusion constant or theoretical plate height, as given by the Van Deemter equation[2], and gaussian peaks result. Aside from Giddings' probabilistic method[1,3], most of the more sophisticated approaches have led to formidable mathematical expressions which were not evaluated numerically. A recent paper of ours[4] dealt with the problem of the rate of mass transfer by means of a time constant and Fourier transform methods, but with this approach it is necessary to assume that the gas velocity and gaseous diffusion are independent of distance along the column.

The major problem in the computation of GLC line shapes from the diffusion equation for a moving gas stream is that of including non-equilibrium effects in the transport of solute between the stationary and moving phases. Inclusion of these leads to a pair of coupled partial differential equations the solutions to which involve rather messy double integrals of Bessel functions[5]. Still, analysis of the problem by means of the differential equations for diffusion readily permits inclusion of spatial variations in gas flow-rate and molecular diffusion constant, and variation of distribution coefficient with solute concentration if the isotherm is non-linear.

A very general analysis of the line shape problem has been given by Giddings, who used a stochastic approach[1,3,6–9]. Yamazaki[10] and Kocirik[11] have used moment analysis on non-equilibrium GLC line shapes and Houghton[12] has used perturbation methods for handling diffusion and non-equilibrium mass transport effects. Vink[13,14] has computed line shapes by a mesh technique for solving the partial differential equations and Olson[15] has investigated the contribution of carrier gas expansion in the column to peak width.

We present here results obtained by a pair of methods which take into account non-equilibrium in mass transport between phases and the variation of gas velocity and diffusion constant along the length of the column. The differential equations are solved by straightforward numerical techniques. Plots of peaks are given for a number of values of the various parameters affecting line shape.

ANALYSIS

Here we outline two different approaches for developing reasonably tractable differential equations governing line shapes in GLC. Let

K = distribution coefficient of solute between solvent and vapor phase
x = distance from inlet end of column
$v(x)$ = carrier gas velocity at point x.
$c_g(x,t)$ = gas phase solute concentration at point x and time t
$c_l(x,t)$ = liquid phase solute concentration at point x and time t
$D(x)$ = effective gaseous diffusion constant.
$B\mathrm{d}x$ = volume of liquid phase between x and $x + \mathrm{d}x$.
$A\mathrm{d}x$ = volume of vapor phase between x and $x + \mathrm{d}x$.

We shall examine the material balance for the volume element dx over a time dt. One approach, discussed in detail in our earlier paper[4], introduces non-equilibrium between the liquid and the vapor phases by simply setting

$$c_l(x,t) = Kc_g(x,t - \tau) \tag{1}$$

where τ is a time constant associated with the delayed response of the concentration of solute in the liquid to the concentration in the vapor. The usual type of material balance analysis then yields

$$\frac{\partial}{\partial x}\left[D\frac{\partial c_g - vc_g}{\partial x}\right] = \frac{\partial c_g}{\partial t} + \frac{BK}{A}\frac{\partial c_g(x,t - \tau)}{\partial t} \tag{2}$$

Expanding the second term on the right in a Taylor's series in powers of τ and dropping terms above those linear in τ yields

$$\frac{\partial}{\partial x}\left[D(x)\frac{\partial c_g}{\partial x} - vc_g\right] = \left(1 + \frac{BK}{A}\right)\frac{\partial c_g}{\partial t} - \frac{BK\tau}{A}\cdot\frac{\partial^2 c_g}{\partial t^2} \tag{3}$$

This partial differential equation is then approximated by the following system of difference equations

$$
\begin{aligned}
c_g(n,m+1) = c_g(n,m) - \frac{\beta}{\alpha}\Big[c_g(n,m) - c_g(n,m-1)\Big] + \\
+ \frac{\Delta t}{\alpha}\Big\{- \frac{v(n)}{\Delta x}\, c_g(n,m) + \frac{v(n-1)}{\Delta x}\, c_g(n-1,m) + \\
+ \frac{D(n)}{(\Delta x)^2}\Big[c_g(n+1,m) - c_g(n,m)\Big] - \frac{D(n-1)}{(\Delta x)^2}\Big[c_g(n,m) - c_g(n-1,m)\Big]\Big\}
\end{aligned}
$$

where

$$
\begin{aligned}
\alpha &= \left(1 + \frac{BK}{A} - \frac{BK\tau}{\Delta tA}\right) \\
\beta &= \frac{BK\tau}{\Delta tA} \\
c_g(n,m) &= c_g(n\Delta x, m\Delta t), \text{ etc.}
\end{aligned}
\qquad (4)
$$

Solute-absorbing barriers were assumed at both ends of the column —$c(1,m) = c(n_f,m) = 0$ for all m)— and the initial distribution of solute was taken to be $c(4,0) =$ const., $c(n,0) = 0$, $n \neq 4$. A modification of eqn. 4 made use of a simple predictor–corrector method[16], but this refinement does not seem to be needed.

Eqn. 4 was found to yield excellent results provided that τ was less than Δt. If this condition was not met, drastic instabilities arose in the solution, so this approach, unlike our earlier Fourier transform method, is limited to small departures from equilibrium. A number of modifications in our method of approximating eqn. 3 failed to overcome this difficulty.

An alternative approach follows which lends itself to large departures from equilibrium in the mass transport between the liquid and vapor phases. The material balance equation for the volume element of column between x and $x + dx$ is

$$
A\frac{\partial c_g}{\partial t} + B\frac{\partial c_l}{\partial t} = -A\frac{\partial}{\partial x}(vc_g) + A\frac{\partial}{\partial x}\left(D\frac{\partial c_g}{\partial x}\right) \qquad (5)
$$

We take as the rate equation governing mass transport between phases the following:

$$
\frac{\partial c_g}{\partial t} = k_1(K^{-1}c_l - c_g) \qquad (6)
$$

We solve eqn. 6 approximately in the time interval $(t_1, t_1 + \Delta t)$ by neglecting the flow of solute into the volume element dx via the gas phase. This leads to the following results:

$$
c_g(n,m\Delta t + \delta t) = [c_g(n,m) - c_g^{\infty}(n,m)]\exp(-k_1\delta t) + c_g^{\infty}(n,m) \qquad (7)
$$

where

$$
k_1 = k_1'(1 + K^{-1}AB^{-1})
$$

and a similar equation for $c_l(n,m\Delta t + \delta t)$.

$$
A\, c_g(n,m) + B\, c_l(n,m) = A\, c_g^{\infty}(n,m) + B\, c_l^{\infty}(n,m) \qquad (8)
$$

$$
K = \frac{c_l^{\infty}(n,m)}{c_g^{\infty}(n,m)} \qquad (9)
$$

From eqns. 8 and 9 we find

$$
\begin{aligned}
c_l^{\infty}(n,m) &= \frac{K[A\,c_g(n,m) + B\,c_l(n,m)]}{A + BK} \\
c_g^{\infty}(n,m) &= \frac{A\,c_g(n,m) + B\,c_l(n,m)}{A + BK}
\end{aligned}
\tag{10}
$$

The net flow of solute into the volume element Δx is given by integrating eqn. 5 from $m\Delta t$ to $(m + 1)\Delta t$, using eqn. 7 for $c_g(n,m\Delta t + \delta t)$ on the right-hand side. This yields

$$
\begin{aligned}
&A[c_g(n,m + 1) - c_g(n,m)] + B[c_l(n,m + 1) - c_l(n,m)] = \\
&\quad = A\left\{-\frac{\partial}{\partial x}\,v + \frac{\partial}{\partial x}\,D\,\frac{\partial}{\partial x}\right\}\cdot\Big\{k_1^{-1}\,[1 - \exp(-k_1\Delta t)]\cdot \\
&\qquad \cdot[c_g(n,m) - c_g^{\infty}(n,m)] + c_g^{\infty}(n,m)\Delta t\Big\}
\end{aligned}
\tag{11}
$$

The differential operator on the right-hand side of eqn. 11 is then approximated by finite differences as in eqn. 4 to yield

$$
\begin{aligned}
c_g(n,m + 1) = {}& u\left[\frac{v(n - 1)}{\Delta x} + \frac{D(n - 1)}{(\Delta x)^2}\right] c_g(n - 1,m) + \\
&+ (\Delta t - u)\left[\frac{v(n - 1)}{\Delta x} + \frac{D(n - 1)}{(\Delta x)^2}\right] c_g^{\infty}(n - 1,m) + \\
&+ \left\{1 - u\left[\frac{-v(n)}{\Delta x} - \frac{D(n) + D(n - 1)}{(\Delta x)^2}\right]\right\} c_g(n,m) + \\
&+ (\Delta t - u)\left[\frac{-v(n)}{\Delta x} - \frac{D(n) + D(n - 1)}{(\Delta x)^2}\right] c_g^{\infty}(n,m) + \\
&+ u\,\frac{D(n)}{(\Delta x)^2}\,c_g(n + 1,m) + (\Delta t - u)\,\frac{D(n)}{(\Delta x)^2}\,c_g^{\infty}(n + 1,m) + \\
&+ (B/A)\,c_l(n,m) - (B/A)\,c_l(n,m + 1)
\end{aligned}
\tag{12}
$$

where

$$u = k_1^{-1}\,[1 - \exp(-k_1\Delta t)]$$

Here $c_l(n,m + 1)$ is given by the analog to eqn. 7,

$$c_l(n,m + 1) = [c_l(n,m) - c_l^{\infty}(n,m)]\exp(-k_1\Delta t) + c_l^{\infty}(n,m) \tag{13}$$

Eqns. 10, 12, and 13 are then solved by computer with a δ-function concentration pulse at the column input at time zero.

It was found that this approach gave line shapes which passed to the correct limit as k_1, the rate constant for mass transport between phases, became very large, and that for rather large k_1 this method gave results in agreement with those obtained from eqn. 4. Typical execution times on the XDS Sigma 7 computer of the Vanderbilt Computer Center were about 3.5 min.

In both eqns. 4 and 12 it is necessary to calculate the gas velocity and the diffusion constant at various points along the length of the column. This was done as follows. The gas is assumed ideal, so that

$$P(x)\, v(x)\, A = \Delta n R T \tag{14}$$

where Δn is the molar flux of gas in the column and $P(x)$ is the pressure at x. We assume that

$$\frac{\mathrm{d}P}{\mathrm{d}x} = -\kappa v^{\beta} \tag{15}$$

where κ and β are constants. From eqns. 14 and 15 one can readily show that

$$P(x) = P_1 \left\{ 1 - [1 - (P_2/P_1)^{\beta+1}] \frac{x}{L} \right\}^{\frac{1}{\beta+1}} \tag{16}$$

where P_1 is the inlet pressure, P_2 is the outlet pressure, and L is the length of the column. The velocity is then conveniently given by

$$v(x) = C_2 \left(1 - \frac{C_1 x}{L} \right)^{\frac{-1}{\beta+1}} \tag{17}$$

where

$$C_1 = 1 - w^{\beta+1}$$

$$C_2 = \frac{(\beta + 1) L}{(\beta + 2) t_2} \cdot \frac{1 - w^{\beta+2}}{1 - w^{\beta+1}}$$

$$w = \frac{P_2}{P_1}$$

Here t_2 is the time required for a portion of carrier gas to traverse the length of the column.

The gaseous diffusion constant is calculated by eqn. 18 (ref. 17):

$$D(x) = 0.746 \times 10^{-2} (\sigma_1 + \sigma_2)^{-2} \left(\frac{M_1 + M_2}{M_1 M_2} \right)^{1/2} \frac{T^{3/2}}{P(x)} \tag{18}$$

where σ_1 and σ_2 are collision diameters in Å of the carrier and the solute, M_1 and M_2 are their molecular weights in atomic mass units (a.m.u.), $P(x)$ is given in atm, T is in °K, and $D(x)$ is in c.g.s. units.

The dependence of pressure on position x along the column was determined experimentally using a 7.5 ft. (228.6 cm) × ¼ in. (6.35 mm) I.D. column packed with Polypak, 80–120 mesh. Pressures were measured at 1.5-ft. (45.72-cm) intervals when helium was forced through the column at various inlet pressures P_1. The outlet pressure P_2 to which the system was vented was 1 atm, and the temperature was 25°C.

As seen in Fig. 1, the pressure gradients are constant to within the limit of experimental error. We therefore set $\beta = 0$ in the numerical calculations which follow.

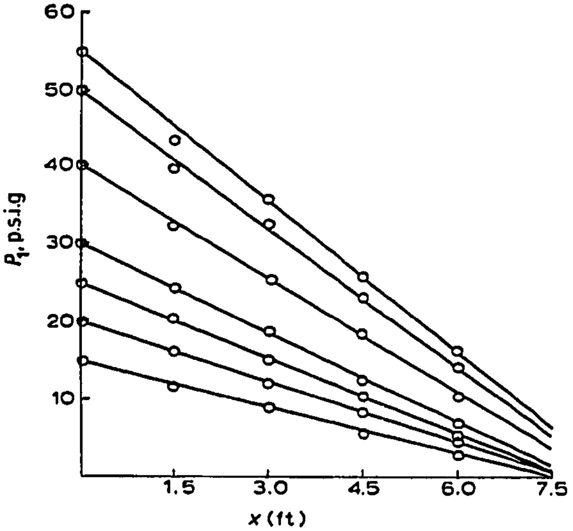

Fig. 1. Pressure in a packed column as a function of distance along the column.

RESULTS

The effect of varying K, the Henry's law constant of the solute, is seen in Fig. 2. The mean retention times calculated from eqn. 19,

$$t_R = t_2(1 + KB/A) \tag{19}$$

are 180 and 210 sec for these two runs; we find a slight displacement to shorter times of the peak maxima. The ratio of retention times calculated from eqn. 19 is 1.167; the ratio of the retention times of the runs plotted in Fig. 2 is 1.168.

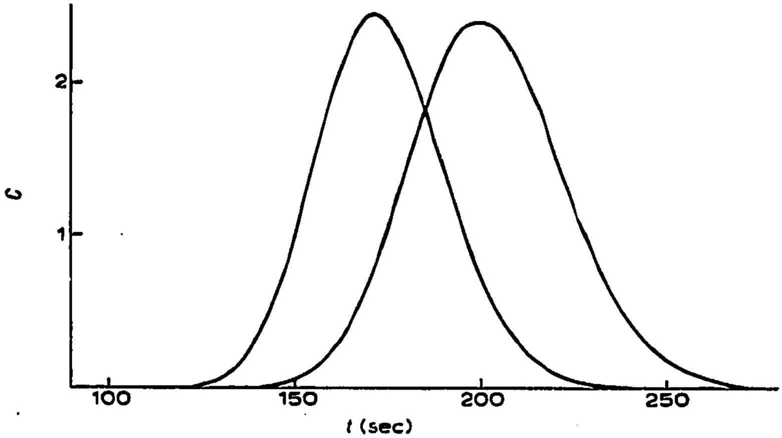

Fig. 2. Dependence of line shape upon the Henry's law constant for the solute, $K = 20$ for the left peak, $K = 30$ for the right one. $A = 1$ cm², $B = 0.1$ cm², $k_1 = 75$ sec⁻¹, $M_1 = 28$ a.m.u., $M_2 = 86$ a m.u., $\sigma_1 = 3$ Å, $\sigma_2 = 5$ Å, $T = 473$°K, $t_2 = 60$ sec, $P_1 = 2.5$ atm, $P_2 = 1.0$ atm, $\beta = 0.0$, $L = 100$ cm.

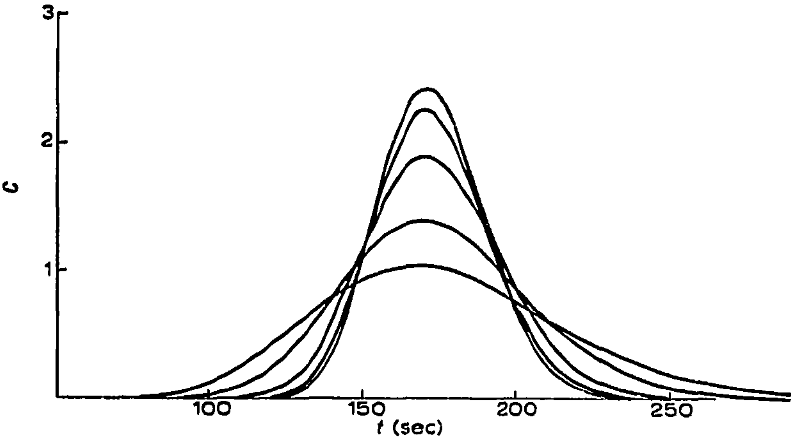

Fig. 3. Dependence of line shape upon the adsorption–desorption rate constant k_1. $K = 20$; $k_1 =$ 75, 50, 25, 10, and 5 sec^{-1} (from the top down); other parameters, as in Fig. 2.

The effect of varying the rate constant for mass transport between phases, k_1, is illustrated in Fig. 3. As one would expect, decreasing values of k_1 result in progressively broader peaks. As with Fig. 2, and as seen in our earlier, simpler model[4], the lines are asymmetric, showing tailing to the right.

The mass of the carrier gas molecules exerts an appreciable effect, as indicated by the peaks in Fig. 4. Hydrogen as a carrier gas is seen to yield somewhat broader peaks than nitrogen, as one would expect.

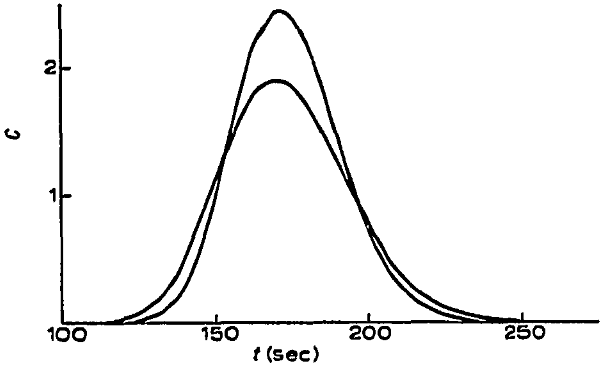

Fig. 4. Effect of changing carrier gas molecular weight m_1 on line shape. $m_1 = 28$ for the narrow curve, $m_1 = 2$ for the broader curve; $K = 20$; other parameters, as in Fig. 2.

The Van Deemter equation[2] expresses the equivalent theoretical plate height, H, as the sum of a term proportional to velocity (mass transport between phases), one independent of velocity (eddy diffusion), and one proportional to the inverse of the velocity (molecular diffusion). The standard deviation of a peak about its center is given by

$$\sigma = \sqrt{HL} \tag{20}$$

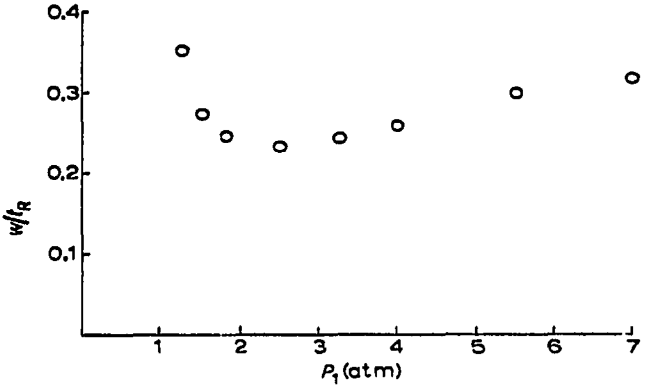

Fig. 5. Half width (w) divided by retention time (t_R) *versus* P_1; $t_2 = 60 \times 1.5/(P_1 - P_2)$ sec; other parameters, as in Fig. 2.

In Fig. 5 we plot half width divided by retention time (an excellent measure of resolution) *versus* inlet pressure; and in Fig. 6 is shown the square of this quantity (proportional to H) as a function of inlet pressure. Evidently these results are of the form indicated by the Van Deemter equation.

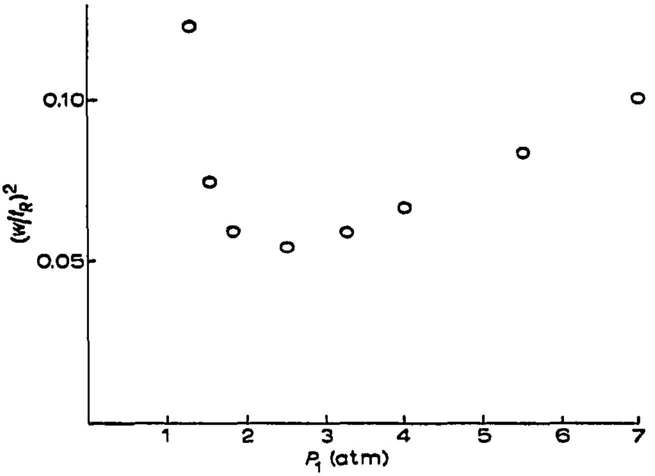

Fig. 6. $(w/t_R)^2$ *versus* P_1. Conditions, same as in Fig. 5.

We were concerned about the extent to which β (see eqn. 15) influences line shapes. Experimentally β is approximately zero. Fig. 7 compares two computed peaks for which β was set equal to 0 and 1, respectively. It is quite apparent from these two runs that minor variations in β would result in no significant changes in line shape, and that we may set $\beta = 0$ with confidence.

For frontal analysis a constant source term is added to the right side of eqn. 12 for $n = 1$, and the initial conditions are taken to be $c_g(n,1) = c_l(n,1) = 0$. Fig. 8 shows

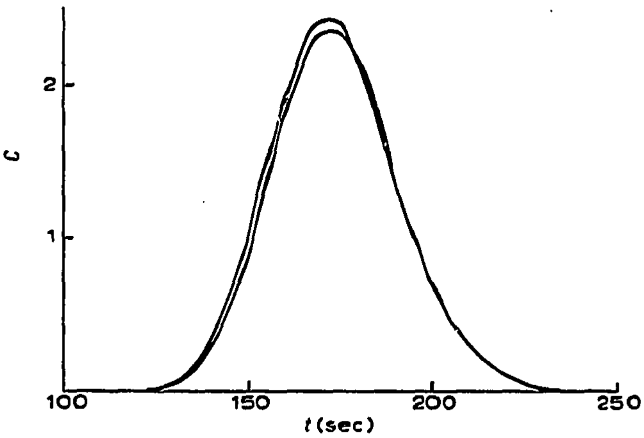

Fig. 7. Dependence of line shape upon β. $\beta = 0.0$ for the upper curve, $\beta = 1.0$ for the lower; other parameters, as in Fig. 2.

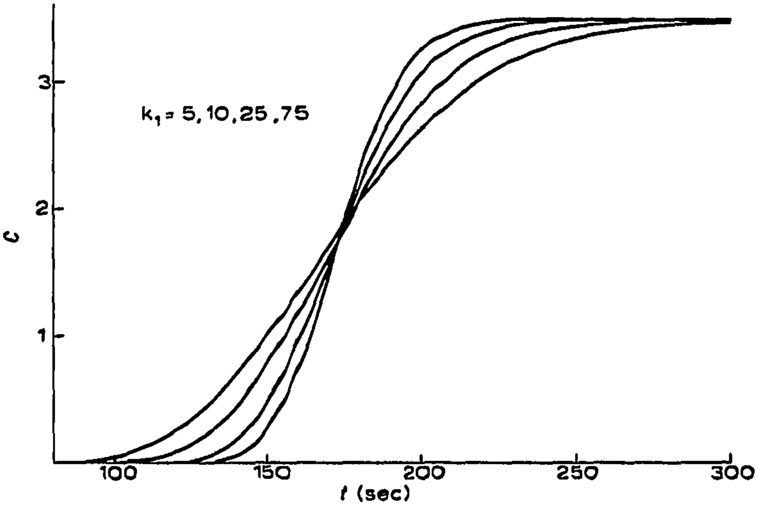

Fig. 8. Frontal analysis. Dependence of line shape upon the adsorption–desorption rate constant k_1. $K = 20$; other parameters, as in Fig. 2.

the effect of varying the rate coefficient for mass transport between phases, and exhibits the expected marked broadening of the front with decreasing rate coefficient. Fig. 9 demonstrates that the value of β chosen in the pressure gradient formula (eqn. 15) does not cause any major changes in the shapes of the fronts.

The effects of the length of time during which the sample is injected can readily be determined by adding an appropriate source term to the right side of eqn. 12 for $n = 1$; we chose square pulses of varying durations. The effects of length of injection interval are clearly seen in Fig. 10. The expected marked deterioration in resolution is observed, and the retention time is seen to increase by one-half the injection interval, as expected.

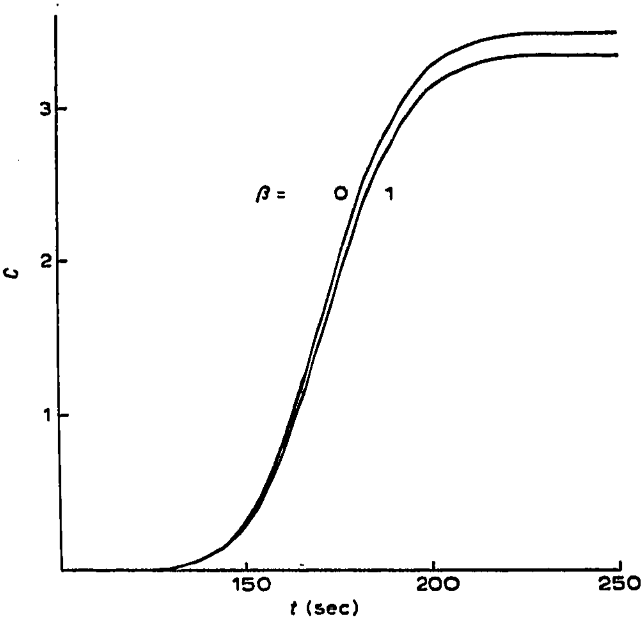

Fig. 9. Frontal analysis. Dependence of line shape upon β, as indicated. $K = 20$; other parameters, as in Fig. 2.

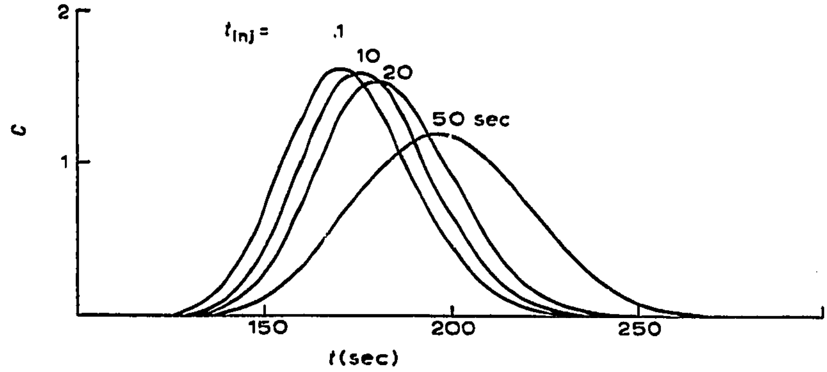

Fig. 10. Effect of injection period, as indicated; t_{inj} is the duration of the square wave injection. $K = 20$; other parameters, as in Fig. 2.

The effects of non-linear isotherms ($K = K_0 + K'c_l$) are shown in Figs. 11 and 12. In Fig. 11 we see the results of varying K'; depending on its sign and magnitude the curves may show tailing on either side. Fig. 12 shows the effects on line shape and retention time of varying the sample size for a particular non-linear isotherm. Our choice of an expression for K which is linear in c_l leads to a roughly linear dependence of the retention time on the height of the peak maximum. (The retention time for vanishingly small samples here is 172 sec.) To the extent that our linear approximation for K is warranted in reality, simple linear extrapolation of retention times to zero concentration would appear valid.

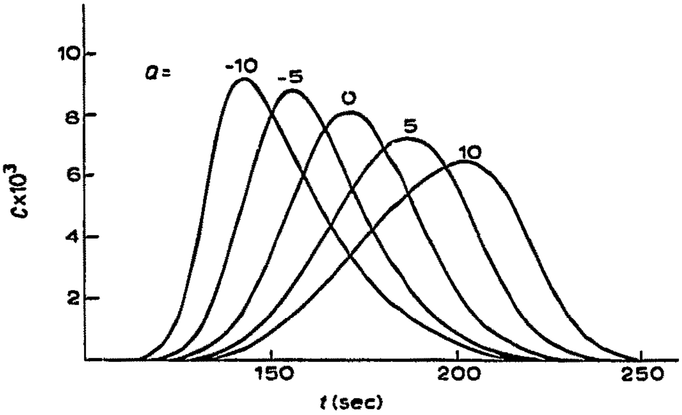

Fig. 11. Non-linear chromatography effect of non-linear isotherms on line shape and retention time. $K = 20 + QC$; Q, as indicated; other parameters, as in Fig. 2.

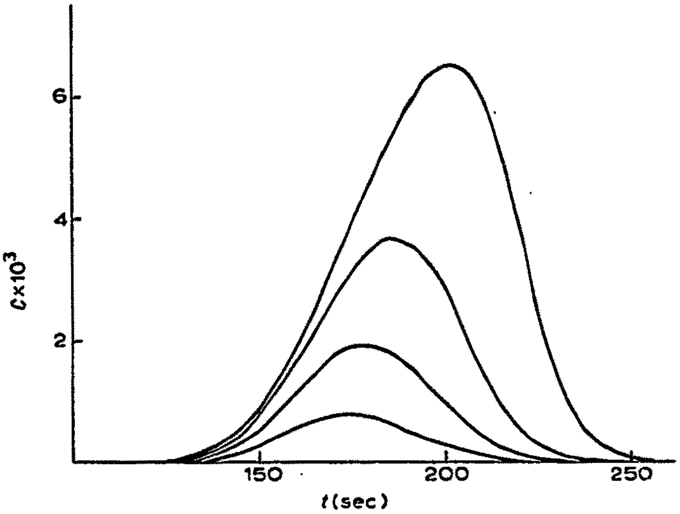

Fig. 12. Effect of variation in sample size on line shape in non-linear chromatography. $K = 20 + 10c_l$, other parameters, as in Fig. 2.

ACKNOWLEDGEMENT

We are indebted to Mr. Douglas Wilhelm for the experimental measurements of the pressure gradients in chromatographic columns.

REFERENCES

1 J. C. Giddings, *Dynamics of Chromatography*. Part I. *Principles and Theory*, Marcel Dekker, New York, 1965.
2 J. J. van Deemter, F. J. Zuiderweg and A. Klinkenberg, *Chem. Eng. Sci.*, 5 (1956) 271.
3 J. C. Giddings and H. Eyring, *J. Phys. Chem.*, 59 (1955) 416.
4 J. P. Muth, D. J. Wilson and K. A. Overholser, *J. Chromatogr.*, 87 (1973) 1.

5 L. Lapidus and N. R. Amundson, *J. Phys. Chem.*, 56 (1952) 984.
6 J. C. Giddings, *J. Chem. Phys.*, 26 (1957) 1755; 31 (1959) 1462.
7 J. C. Giddings, *J. Chromatogr.*, 1 (1963) 38; 2 (1959) 44.
8 J. C. Giddings, *Anal. Chem.*, 33 (1961) 962; 34 (1962) 458, 722, 1186; 35 (1963) 439.
9 J. C. Giddings, *J. Phys. Chem.*, 68 (1964) 184.
10 H. Yamazaki, *J. Chromatogr.*, 27 (1967) 14.
11 M. Kocirik, *J. Chromatogr.*, 30 (1967) 459.
12 G. Houghton, *J. Chromatogr.*, 15 (1964) 5.
13 H. Vink, *J. Chromatogr.*, 20 (1965) 496.
14 H. Vink, *J. Chromatogr.*, 24 (1966) 39.
15 J. H. Olson, *J. Chromatogr.*, 27 (1967) 1.
16 L. Fox, *Numerical Solution of Ordinary and Partial Differential Equations*, Addison-Wesley, Reading, Mass., 1962, pp. 28–32.
17 R. D. Present, *Kinetic Theory of Gases*, McGraw-Hill, New York, 1958, p. 149.